ICASSP 2024 - 2024 IEEE International Conference on Acoustics, Speech and Signal Processing (ICASSP) | 979-8-3503-4485-1/24/$31.00 ©2024 IEEE | DOI: 10.1109/ICASSP48485.2024.10448323

ENABLING ORIENTATION-FREE MMWAVE-BASED VITAL SIGN SENSING WITH MULTI-DOMAIN SIGNAL ANALYSIS

*Hanqin Gong, *Dongheng Zhang, Jinbo Chen, Yadong Li, Guixin Xu, Yuqin Yuan, Yang Hu, Yan Chen*

University of Science and Technology of China, Hefei, China

ABSTRACT

Contactless vital signs estimation using mmWave radar has gained significant attention. However, existing studies are built upon the radar being directed facing the thorax to capture fine-grained vital signs, ignoring the angle variation between the radar and thorax in practical deployment. In this paper, we propose a spatial-temporal optimization model to estimate the human body orientations between the radar and thorax through extracting the multi-domain features of reflected signal. By aligning the signal variation captured from different angles, we can realize orientation-free vital sign sensing. The system achieves an average angle estimation error of 13.1°, and a 14.8% discrepancy reduction in terms of the mean absolute error of the signal captured at different angles.

Index Terms— Wireless sensing, millimeter wave radar, vital signs, body orientation

1. INTRODUCTION

Long-term monitoring of human respiration and heartbeat is significant for medical diagnosis of lung and cardiovascular diseases, as well as the evaluation of sleep status [1, 2]. However, existing monitoring systems typically rely on intrusive sensors [3, 4], which leads to discomfort for patients. To address these challenges, non-contact vital sign sensing using radio signals has gained significant attention due to its ability to extract phase variations caused by chest movements and heart beats without the need for physical contact [5, 6, 7]. Existing studies often require the human chest to face the radar directly [8, 9], as this position yields the most pronounced and easily extractable chest movement. However, when the angle between the body and the radar changes, the modulation of the reflected signal by the thoracic micromotion becomes weaker, which may lead to incorrectly interprets the situation as hypoventilation [2], or the wrong results to the measurement of human lung capacity [10].

The key to addressing this issue lies in accurately determining the body orientation [11]. Several research efforts have been devoted to this area. For instance, in [12], they utilize radar arrays at three different locations and a random forest algorithm to classify six orientations of the human body. Similarly, [13] utilizes four radar arrays at different locations to capture the Doppler features of waving arms for classifying the eight orientations of human body. In [14], a distributed radar network with a radius of 1.3 m is employed to estimate the respiration rate and heart rate of human subjects located at different orientations. While these approaches address this issue to some extent, they rely on multiple radar devices located at different locations, which increases the system cost and hardware complexity. Additionally, they simply treat the body orientation estimation as a classification problem, and cannot obtain specific angles.

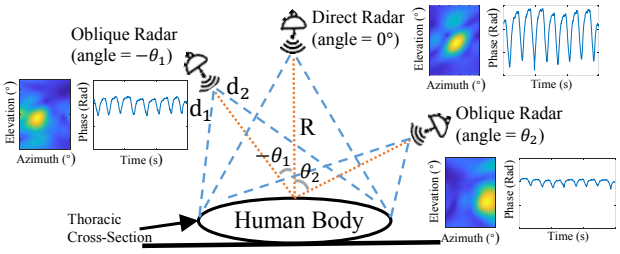

Fig. 1. Impact of body orientation on the phase variations.

In this paper, we present a novel framework for estimating the human body orientations and aligning signal phase variation at various body orientations using a single-chip millimeter-wave radar. Our key design principle is to extract signal features related to body orientations from different domains. To achieve this, we first implement a 4D chest imaging algorithm to locate the human body (specifically the chest). Then, we analyze and capture signal features from the spatial domain, frequency domain, and energy domain. These features reflect the correlations between the signal variations and body orientations. Based on the extracted features, we formulate the angle estimation as an optimization problem to obtain the body orientations. Finally, we leverage the estimated angles to compensate for the phase variation of the reflected signal. Extensive experiments have demonstrated that our approach can achieve an average angle estimation error of 13.1°, and after compensation, the absolute phase error between oblique and direct signals is reduced by 14.8%.

*Dongheng Zhang is the corresponding author. This work was supported by National Key R&D Programmes under Grant 2022YFC2503405, National Natural Science Foundation of China under Grant 62201542

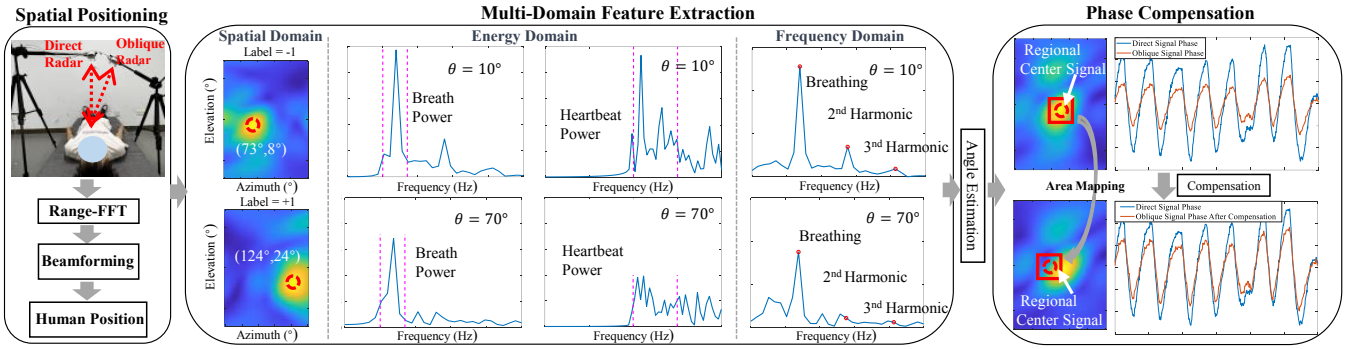

Fig. 2. The proposed system consists of three components: spatial positioning, multi-domain feature extraction and phase compensation. Firstly, our system locates the human target using a series of array signal processing methods. Subsequently, we extract eight features that contain body orientation information from the spatial, energy, and frequency domains of the signal. These features are then utilized to estimate the specific angle with an optimized model. Finally, we leverage the angle information to compensate for the phase of the oblique signal.

2. METHOD

As shown in Fig. 2, our proposed approach encompasses the following steps: (1) identifying the spatial position to locate the target, (2) conducting multi-domain feature extraction and angle estimation, and (3) compensating for signal phases across different orientations.

2.1. Spatial Positioning and Signal Modeling

The reflected signals from the human body's chest carry the information about chest motion, where changes in the distance between the chest cavity and radar significantly modulate the signal phase:

$$\phi(t) = 2\pi \frac{d(t)}{\lambda}, \tag{1}$$

where λ is the wavelength of the Radio Frequency (RF) signals, $d(t)$ is the distance between the radar sensor and reflection position, and t is sensing time.

With a 2D antenna array and Frequency-Modulated Continuous Wave (FMCW), we can obtain RF reflections in 3D space [8, 15]. Specifically, as shown in Fig. 2 , we first perform range-FFT on the reflected signals and localize the human body by finding the range bin with the highest reflected energy [16]. Then, we perform 2D beamforming on the received signal from the selected range bin [17, 18, 19], obtaining the differentiated representation of each voxel in the 2D plane (azimuth and elevation directions) [20].

When the human body faces the radar, chest movement produces the strongest modulation on the radar signal. However, when the human chest forms a certain angle with the radar, the modulation of the signal by chest movement will be the projections of the radar beam direction:

$$\begin{aligned} S_d(t) &= B(t)S(t)e^{j2\pi\frac{2d(t)}{\lambda}} \\ S_o(t) &= A(\theta)B(t)S(t)e^{j2\pi\frac{2d(t)\gamma\cos(\theta)}{\lambda}}, \end{aligned} \tag{2}$$

where $S_d(t)$ is the direct radar reflected signal, $S_o(t)$ is the oblique radar reflected signal, $S(t)$ is the radar transmitted signal, $B(t)$ represents the modulation of the signal amplitude under direct conditions, $A(\theta)$ represents the further modulation of the signal amplitude at θ degrees beyond the direct condition, $d(t)$ is the thoracic heave distance, and $\gamma cos(\theta)$ represents the projection coefficients. From Eq. 2, we can see that the phase of the oblique signal can be compensated by solving the angle θ.

2.2. Multi-Domain Feature Extraction

From Eq. 2, we see that both the amplitude and phase of the received signal are affected by the angle θ. Thus, we aim to obtain angle information by extracting these angle-related features.

Spatial domain. Firstly, we extract the target's spatial distribution in the radar coordinate system (shown by the blue dotted line in Fig. 1). The distribution of the human body in the radiation area changes with the orientation. At $\theta = 0°$, the human body is directly beneath the radar, with nearly symmetrical irradiation range on the left and right. This can also be seen in the heatmap of beamforming, where the target is centrally located. For $\theta \neq 0°$, the radar-to-right-chest distance are not equal to the radar-to-left-chest distance, causing an overall shift of the target position in the heatmap. Therefore, despite the radar's limited resolution preventing us from determining the precise orientation, this feature helps discern if the human body is towards left or right.

Frequency domain. Breathing is the predominant cause of chest movement at rest, which extensively modulates the phase of reflected signals. This modulation results from both

chest motion and the orientations between the human body and radar, with angle information also being included in the signal amplitude. Hence, our analysis focuses on extracting the most pronounced respiratory component. Specifically, the received signal, after passing through a band-pass filter, will show a spike in the respiratory frequency range of 0.2-0.34 Hz (12-20 bpm) [21], which represents the fundamental frequency of the respiratory signal. This information allows us to identify the second and third harmonics of the respiratory frequency [22], which correspond to amplitudes that characterize respiration, as depicted in Fig. 2.

Energy domain. To enhance model generalization, we consider low signal-to-noise ratio environments where noise might affect the distribution of signal spectrum. Therefore, instead of relying solely on a single respiratory frequency that may be contaminated by the noise, we partially preserve the modulation information by calculating the total energy within the frequency band containing human respiration and heartbeat. Specifically, we apply a band-pass filter of 0.2-0.34 Hz (12-20 bpm) and a band-pass filter of 1-1.5 Hz (60-90 bpm) [23] to the raw signals. By doing so, we can calculate the total energy within the respiration band and the heartbeat band, respectively, as shown by the pink dashed line in Fig. 2.

In summary, we derive eight features in total for estimating the orientation of the human body: the elevation and azimuth angles of the strongest reflection point, the fundamental amplitude of the respiratory signal, the second harmonic amplitude, the third harmonic amplitude, the total energy of the respiratory band, the total energy of the heartbeat band, and the left/right rotation label obtained from azimuth angle discrimination. We can represent these as a feature vector $\boldsymbol{x}$:

$$\boldsymbol{x} = [1, x_1, x_2, x_3, x_4, x_5, x_6, x_7, x_8]\,. \tag{3}$$

We model the optimization problem for angle estimation as follows:

$$\boldsymbol{\omega}^* = \underset{\boldsymbol{\omega}}{arg\,min} \sum_{n=1}^{N} \left|\left|\theta_n - \boldsymbol{\omega}\, \boldsymbol{x}_n^T\right|\right|_2^2, \tag{4}$$

where n is the n-th set of data, θ_n is the true angle corresponding to the n-th set of signal data, and $\boldsymbol{x}_n$ is the feature corresponding to the n-th set of signal data. Therefore, the angle estimation results can be expressed as $\hat{\theta} = \boldsymbol{\omega}\boldsymbol{x}^T$ and vector $\boldsymbol{\omega}$ is the weight distribution of each feature.

2.3. Adaptive Compensation of Signal Phase

Based on the angular information obtained, we can compensate for the signal phase in the radar oblique state.

Firstly, we locate both the oblique and direct signals from the same region of the human body's surface through inter-area correlation. Taking the location of the strongest energy reflection of the received oblique signal as the center, we frame an approximated 9.1 cm $\times$ 9.1 cm area (10° elevation and azimuth angle). By using a sliding window to traverse the direct signal's perception range, we can compute the inter-area cross-correlation, defined as the sum of all signal phases cross-correlations. Ultimately, the range with the largest cross-correlation is considered from the same body surface region as the oblique signal's framing range. Results are depicted in Fig. 2.

As can be seen from Eq. 2, for the signal phase modulation caused by the same region, the oblique signal phase is the projection of the direct signal phase at angle multiplied by the attenuation factor γ. Hence, the phase compensation can be realized by the inverse operation of the oblique signal phase. We set the empirical value of attenuation factor γ to $\frac{5}{6}$.

3. EXPERIMENTS

3.1. Experimental Setup

Considering the common ECG monitoring and sleep monitoring scenarios in hospitals, we perform contactless data acquisition in clinically relevant scenarios. As shown in Fig. 3, during data acquisition, the subject is in a supine position on the bed and remain in a quasi-static state. Two radar sensors are placed on a fixed bracket. Direct radar is positioned 0.52 meters above the chest's center, while the oblique radar is situated 0.52 meters lateral to the chest's center and angled to capture the movements of the thoracic cavity from different perspectives. We conduct a total of 98 experiments involving 7 participants aged between 21 and 25 years, including 5 males and 2 females. In each experiment, the angle between the oblique radar and the human body is adjusted by 10 degrees and each session is conducted for a duration of 40 seconds and is repeated three times.

We implement our contactless ECG monitoring system by using TI IWR6843 millimeter-wave radar and DCA1000 real-time data acquisition board. We activate 3 transmitters (Tx) and 4 receivers (Rx) to achieve a virtual 2D antenna array with 12 channels. The radar operates within a frequency band of 60-64 GHz and has a sampling rate of 100 Hz. The 3D beamforming is carried out in the radar's relative coordinates. Considering the radar's beam sensing range and detection distance, we refine the 3D sensing grid into 15 range bins, 40°-140° azimuth angles, and -70°-70° elevation angles.

3.2. Evaluation Metrics

In the first part of angle estimation, we input radar signals gathered from different angles to estimate angle information. We utilize the Mean Absolute Error (MAE) as a metric:

$$MAE = \frac{1}{N}\sum_{n=1}^{N}(\left|\theta_n - \hat{\theta}_n\right|), \tag{5}$$

where θ is the true angle, $\hat{\theta}$ is the estimated angle, N is the number of tests.

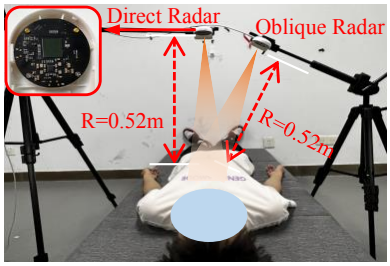

Fig. 3. Experimental setup of data collection.

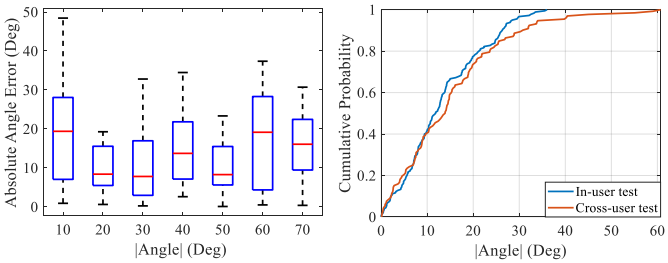

(a) Angle estimation error (b) ECDF of cross-validation

Fig. 4. Cross-validation generalization across individuals.

In the second part, for both the oblique signal phase before and after phase compensation, we compute their MAE with the phase of the direct signal. Then, we use the improvement of these two MAEs to demonstrate the effectiveness of our system.

3.3. Experimental Results

We first evaluate the accuracy of the single chip radar system for orientation estimation.

Our system demonstrates an average accuracy of 98.3% in determining the direction of rotation of the human body, whether it is towards the left or right. Angle estimation tests are performed on 294 sets of time series samples obtained from various subjects at different angles within a range of -70° to 70° of human rotation, and the average angle estimation error is 13.1°, as shown in Fig. 4(a).

In order to verify the generalizability of the algorithm on different users, we use data from 3 random users as the training data and 4 new users as the test data. As shown in Fig. 4(b), our method can well generalize to different users, and only samples from a small number of user is needed to achieve orientation estimation for new users.

Furthermore, we utilize the angle information to compensate for the phase of all signals within the framed region of the oblique signal, and the MAE between the phase of the oblique signal and the phase of the direct signal is reduced by 14.8% before and after the compensation, across various subjects and at different angles. The MAE of phase enhancement capability at each angle is shown in Table 1. This reveals that the phase of the oblique signal has been enhanced after compensation at various different angles. Fig. 5(a) shows the phase distribution of the signal under a 70° oblique radiation condition and the phase portion of the direct radiation condition. It is evident that the change in signal phase under the oblique radiation is much weaker. Fig. 5(b) shows that after phase compensation, the signal phase under the oblique radiation condition is better restored to the direct radiation condition, which reflects a more realistic undulation movement of the chest and reduces the dependence of the non-contact perception on the human body posture.

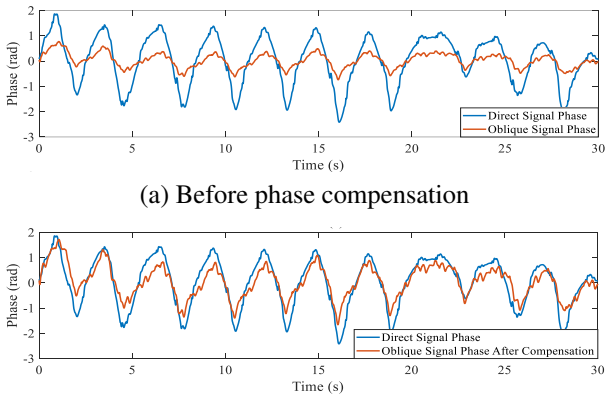

(a) Before phase compensation

(b) After phase compensation

Fig. 5. Signal phase before and after compensation when orientation is 70°.

|Angle|	10°	20°	30°	40°	50°	60°	70°
Improved(%)	13.3	20.4	3.0	4.9	12.2	21.5	28.2

Table 1. Percentage of MAE improvement before and after signal phase compensation at different angles.

4. CONCLUSION

In this paper, we proposed an algorithm for estimating the human body orientations of the radar and the chest cavity using a single millimeter-wave radar. Based on that, we implemented phase compensation for the received signal under oblique incidence conditions. By extracting the multi-domain features of the received signals at different angles, we realized robust orientation estimation through an optimization model and then aligned the signal phase of different orienations. Our method achieved an angle estimation error of 13.1° and reduced the absolute error in the phase of the oblique and direct signals by 14.8%. Through reliable orientation detection and phase compensation, we believe our framework significantly mitigates the stringent posture requirements typically associated with RF-based vital signs monitoring.

5. REFERENCES

[1] Özal Yıldırım, Paweł Pławiak, Ru-San Tan, and U Rajendra Acharya, "Arrhythmia detection using deep convolutional neural network with long duration ecg signals," *Computers in biology and medicine*, vol. 102, pp. 411–420, 2018.

[2] Masayuki Kagawa, Katsuhiko Ueki, Hirokazu Tojima, and Takemi Matsui, "Noncontact screening system with two microwave radars for the diagnosis of sleep apnea-hypopnea syndrome," in *2013 35th Annual International Conference of the IEEE Engineering in Medicine and Biology Society (EMBC)*. IEEE, 2013, pp. 2052–2055.

[3] Mirza Mansoor Baig, Hamid Gholamhosseini, and Martin J Connolly, "A comprehensive survey of wearable and wireless ecg monitoring systems for older adults," *Medical & biological engineering & computing*, vol. 51, pp. 485–495, 2013.

[4] Mohamed Adel Serhani, Hadeel T. El Kassabi, Heba Ismail, and Alramzana Nujum Navaz, "Ecg monitoring systems: Review, architecture, processes, and key challenges," *Sensors*, vol. 20, no. 6, pp. 1796, 2020.

[5] Marco Mercuri, Ilde Rosa Lorato, Yao-Hong Liu, Fokko Wieringa, Chris Van Hoof, and Tom Torfs, "Vital-sign monitoring and spatial tracking of multiple people using a contactless radar-based sensor," *Nature Electronics*, vol. 2, no. 6, pp. 252–262, 2019.

[6] Dongheng Zhang, Yang Hu, and Yan Chen, "Mtrack: Tracking multiperson moving trajectories and vital signs with radio signals," *IEEE Internet of Things Journal*, vol. 8, no. 5, pp. 3904–3914, 2020.

[7] Shujie Zhang, Tianyue Zheng, Zhe Chen, and Jun Luo, "Can we obtain fine-grained heartbeat waveform via contact-free rf-sensing?," in *IEEE INFOCOM 2022-IEEE conference on computer communications*. IEEE, 2022, pp. 1759–1768.

[8] Jinbo Chen, Dongheng Zhang, Zhi Wu, Fang Zhou, Qibin Sun, and Yan Chen, "Contactless electrocardiogram monitoring with millimeter wave radar," *IEEE Transactions on Mobile Computing*, 2022.

[9] Weicheng Wang, Zhenhua Jia, Chenren Xu, Guojie Luo, Daqing Zhang, Ning An, and Yanyong Zhang, "Feasibility study of practical vital sign detection using millimeter-wave radios," *CCF Transactions on Pervasive Computing and Interaction*, vol. 3, pp. 436–452, 2021.

[10] Xingzhe Song, Boyuan Yang, Ge Yang, Ruirong Chen, Erick Forno, Wei Chen, and Wei Gao, "Spirosonic: monitoring human lung function via acoustic sensing on commodity smartphones," in *Proceedings of the 26th Annual International Conference on Mobile Computing and Networking*, 2020, pp. 1–14.

[11] Hojjat Salehinejad, Navid Hasanzadeh, Radomir Djogo, and Shahrokh Valaee, "Joint human orientation-activity recognition using wifi signals for human-machine interaction," in *ICASSP 2023-2023 IEEE International Conference on Acoustics, Speech and Signal Processing (ICASSP)*. IEEE, 2023, pp. 1–5.

[12] Xiuzhu Yang, Yibo Yu, Hongyu Qian, Xinyue Zhang, and Lin Zhang, "Body orientation and vital sign measurement with ir-uwb radar network," in *2020 42nd Annual International Conference of the IEEE Engineering in Medicine & Biology Society (EMBC)*. IEEE, 2020, pp. 485–488.

[13] Yiran Li, Ranadip Pal, and Changzhi Li, "Non-contact multi-radar smart probing of body orientation based on micro-doppler signatures," in *2014 36th Annual International Conference of the IEEE Engineering in Medicine and Biology Society*. IEEE, 2014, pp. 598–601.

[14] Wei Ren, Fugui Qi, Farnaz Foroughian, Tsotne Kvelashvili, Quanhua Liu, Ozlem Kilic, Teng Long, and Aly E Fathy, "Vital sign detection in any orientation using a distributed radar network via modified independent component analysis," *IEEE Transactions on Microwave Theory and Techniques*, vol. 69, no. 11, pp. 4774–4790, 2021.

[15] Yan Chen, Xiang Su, Yang Hu, and Bing Zeng, "Residual carrier frequency offset estimation and compensation for commodity wifi," *IEEE Transactions on Mobile Computing*, vol. 19, no. 12, pp. 2891–2902, 2019.

[16] Fengyu Wang, Xiaolu Zeng, Chenshu Wu, Beibei Wang, and KJ Ray Liu, "mmhrv: Contactless heart rate variability monitoring using millimeter-wave radio," *IEEE Internet of Things Journal*, vol. 8, no. 22, pp. 16623–16636, 2021.

[17] Bin-Bin Zhang, Dongheng Zhang, Yadong Li, Yang Hu, and Yan Chen, "Unsupervised domain adaptation for rf-based gesture recognition," *IEEE Internet of Things Journal*, pp. 1–1, 2023.

[18] Wenxuan Li, Dongheng Zhang, Yadong Li, Zhi Wu, Jinbo Chen, Dong Zhang, Yang Hu, Qibin Sun, and Yan Chen, "Real-time fall detection using mmwave radar," in *ICASSP 2022 - 2022 IEEE International Conference on Acoustics, Speech and Signal Processing (ICASSP)*, 2022, pp. 16–20.

[19] Yadong Li, Dongheng Zhang, Jinbo Chen, Jinwei Wan, Dong Zhang, Yang Hu, Qibin Sun, and Yan Chen, "Towards domain-independent and real-time gesture recognition using mmwave signal," *IEEE Transactions on Mobile Computing*, pp. 1–15, 2022.

[20] Yan Chen, Hongyu Deng, Dongheng Zhang, and Yang Hu, "Speednet: Indoor speed estimation with radio signals," *IEEE Internet of Things Journal*, vol. 8, no. 4, pp. 2762–2774, 2020.

[21] Anne De Groote, Muriel Wantier, Guy Chéron, Marc Estenne, and Manuel Paiva, "Chest wall motion during tidal breathing," *Journal of Applied Physiology*, vol. 83, no. 5, pp. 1531–1537, 1997.

[22] Changzhi Li, Yanming Xiao, and Jenshan Lin, "Experiment and spectral analysis of a low-power ka-band heartbeat detector measuring from four sides of a human body," *IEEE Transactions on Microwave Theory and Techniques*, vol. 54, no. 12, pp. 4464–4471, 2006.

[23] G Ramachandran and M Singh, "Three-dimensional reconstruction of cardiac displacement patterns on the chest wall during the p, qrs and t-segments of the ecg by laser speckle inteferometry," *Medical and Biological Engineering and Computing*, vol. 27, pp. 525–530, 1989.